Published in final edited form as:
J Orthop Res. 2011 September ; 29(9): 1367–1374. doi:10.1002/jor.21370.

TNF is required for the induction but not the maintenance of compression-induced BME signals in murine tail vertebrae: limitations of anti-TNF therapy for degenerative disc disease

M. Owen Papuga[1,2,3], **Edmund Kwok**[4], **Zhigang You**[4], **Paul T. Rubery**[1], **Paul E. Dougherty**[3], **Gloria Pryhuber**[5], **Christopher A. Beck**[6], **Matthew J. Hilton**[1], **Hani A. Awad**[1,2], and **Edward M. Schwarz**[1,7]

[1] The Center for Musculoskeletal Research, University of Rochester, Rochester, NY

[2] Department of Biomedical Engineering, University of Rochester, Rochester, NY

[3] New York Chiropractic College, Seneca Falls, NY

[4] Department of Imaging Sciences, University of Rochester, Rochester, NY

[5] Department of Pediatrics, University of Rochester, Rochester, NY

[6] Department of Biostatistics & Computational Biology, University of Rochester, Rochester, NY

Abstract

While bone marrow edema (BME) is diagnostic of spondyloarthropathy, its nature remains poorly understood. In contrast, BME in ankylosing spondylitis is caused by TNF-induced vascular and cellular changes. To investigate the relationship between chronic compression and TNF signaling in compression induced BME we utilized a tail vertebrae compression model with WT, TNF-Tg and TNFR1&2−/− mice to evaluate: 1) healing following release of chronic compression, 2) induction of BME in the absence of TNFR, and 3) efficacy of anti-TNF therapy. Compression-induced normalized marrow contrast enhancement (NMCE) in WT was significantly decreased 3-fold ($p<0.01$) within 2 weeks of release, while the NMCE values in TNF-Tg vertebrae remained elevated, but had a significant decrease ($p<0.05$) by 6 weeks after the release of compression. TNFR1&2−/− mice were resistant to compression-induced BME. Anti-TNF therapy did not affect NMCE vs. placebo. Histological examination revealed that NMCE values significantly correlated with marrow vascularity and cellularity ($p<0.05$), which account for 76% of the variability of NMCE. Collectively, these data demonstrate a critical role for TNF in the induction of chronic compression-induced BME, but not in its maintenance. Amelioration of BME is achieved through biomechanical stability, but is not affected by anti-TNF therapy.

Keywords

Modic Changes; CE-MRI; Bone Marrow Edema; Anti-TNF Therapy

INTRODUCTION

The lifetime adult prevalence rate for low back pain has been estimated at between 50 and 80% with a point prevalence rate from 15–30%. The variation in prevalence rates have been

[7]To whom correspondence should be addressed: Dr. Edward M. Schwarz, The Center for Musculoskeletal Research, University of Rochester Medical Center, 601 Elmwood Avenue, Box 665, Rochester NY 14642, Phone 585-275-3063, FAX 585-275-1121, Edward_Schwarz@URMC.Rochester.edu.

attributed to differences in type and frequency of surveillance conducted.[1] The management of individuals with chronic low back pain (LBP) is as varied as the supposed underlying causes, yet no one intervention has been shown to be superior to another.[2;3] This leaves LBP as a largely unmet healthcare need. Given the lack of evidence-based medicine to manage LBP, it is imperative that basic research be performed to better elucidate the molecular mechanisms responsible for this condition. However, progress in this field has been stalled by our inability to track the molecular underpinnings associated with chronic degenerative changes in the spine over time in a human population. While tissue samples are available at the time of surgical intervention, the collection of such samples throughout the progression of the degeneration would be detrimental to the patient and therefore untenable. The advancement of MRI technology has made longitudinal studies of those individuals with chronic LBP possible, but the inferred knowledge gained through MRI is not sufficient to understand specific molecular changes. Bone marrow edema (BME) observed on MRI,[4] is associated with chronic LBP and has been commonly referred to by specific "Modic changes."[5;6] The Modic type 1 change (MT1), defined as decreased signal intensity on T1 weighted images and increased signal intensity on T2 weighted images, has been shown to be associated with an inflammatory response in the bone marrow and degeneration of the endplate,[5–7] and has been positively correlated with discogenic pain.[8;9] Modic type 2 changes (MT2), defined as increased signal intensity on T1 weighted images and either isointensity or slight increase in intensity on T2 weighted images, have been shown to be associated with the return of fatty marrow and decreased pain.[6;7] The set of cellular and molecular conditions that leads to the MT2 type change is largely unknown, thus a greater understanding of the recovery process could ultimately lead to a more pointed and effective intervention strategy.

Ankylosing Spondylitis (ASp) is a chronic, inflammatory disease that is characterized by sacroilitis, inflammatory back pain, restricted spinal mobility, peripheral arthritis, spondylitis, and enthsitis.[10;11] Recent treatments of rheumatic diseases, such as ASp, have attempted to disrupt the signaling pathway of a critical cytokine, tumor necrosis factor (TNF), involved in the inflammatory immune response. Development of novel therapeutic agents such as infliximab, etanercept, and adalimumab that bind to TNF rendering it unable to fulfill its role as the apex of the inflammatory signaling pathway, have proven effective in treating inflammatory disease states. It has been shown that this class of drugs is effective in treating both the symptoms of ASp and the inflammation associated with the disease.[12] Moreover, BME observed on contrast enhanced (CE)-MRI in affected vertebrae of ASp patients has been validated as a true biomarker of painful disease, as it correlates with disease severity and amelioration with anti-TNF therapy,[13] and it also is predictive of a patient's ability to return to work.[14] Additionally, histology of retrieval tissue obtained from ASp patients has confirmed the vascular and cellular changes in the bone marrow of affected vertebrae to be the nature of the CE-MRI signals.[15] Thus, while the etiology of ASp is largely different from that of chronic LBP and degenerative disc disease (DDD), the potential role of anti-TNF therapy and the utility of BME as a biomarker in the later, beg further investigation.

Preliminary results involving off-label use of anti-TNF therapy in cases of LBP involving radicular pain and sciatica associated with DDD and disc herniation have had varying success, depending on inclusion criteria, and the route of delivery.[16–21] Perispinal and epidural injections of anti-TNF drugs have been reported to have immediate and long lasting positive effects,[16;22] while subcutaneous,[20] intravenous,[21] and intradiscal[18] delivery of such drugs have had mixed results. Most recently, multicenter, randomized, double-blind, placebo-controlled trial of adalimumab in 265 patients with severe and acute sciatica demonstrated that a short course of subcutaneous anti-TNF therapy resulted in a small effect on leg pain and in significantly fewer surgical procedures.[17] Remarkably, there have been

no preclinical studies to date that have attempted to assess the efficacy of anti-TNF therapy for DDD and its potential mechanism of action for this condition.

For many diseases, animal models play an important role in clarifying pathogenesis and testing new and existing interventions. In the era of translational research, the mouse has emerged as an invaluable animal model based on its remarkable genomic conservation with human, transgenic technology, the availability of molecular probes, and cost effectiveness (money, time, labor). However, the generation of a lumbar spine model in the mouse has been prohibitive due to the highly invasive surgery required; whose side effects often involve paralysis and death. In recognition of this, the rodent tail has evolved as a surrogate model, despite its significant differences from the lumbar spine.[23] Recently, we have expanded this animal modeling to murine caudal vertebrae. We have shown using contrast enhanced MRI (CE-MRI) and corresponding histology to track the progression of DDD and the development of bone marrow edema in both wild type (WT) and TNF-Tg mice a correlation between the MRI signal intensity and the cellular and vascular density in both the chronically compressed WT mice and immune compromised TNF-Tg mice.[24] Based on these results and the potential of anti-TNF therapy for DDD, we tested the hypotheses that: 1) TNF is necessary for the induction of chronic compression-induced BME, and 2) compression-induced BME is ameliorated by release of the load and TNF inhibition.

MATERIALS AND METHODS

Animals and Instrumentation

Recovery experiments were performed on 2-month-old, heterozygous TNF-Tg mice, these mice were bred to over-express levels of the human form of TNF, obtained from Dr. G. Kollias.[25] Also included in the recovery experiments were sex matched wild type C57B/6 (WT) littermate controls. For studies of TNF signaling, 2 month old mice lacking both TNFRI and TNFRII were obtained from Dr. G Pryhuber. TNFRsf1a/1b double null mice were regenerated in a C57BL6/J background by backcross of $TNFRI^{tm1mak/j-/-}$ x $TNFRII^{tm1Mwm/J-/-}$, each bred x 12 onto C57BL/6J prior to interbreeding.[26] These TNFR-deficient (TNFR1&2−/−) mice lack both receptors for TNF and therefore cannot respond to TNF. In the drug intervention studies WT mice, with caudal vertebrae under constant load, received either murine monoclonal anti-mouse TNF IgG1 antibody or an irrelevant murine IgG1 placebo control (Centocor R&D, Radnor, PA) at a dosage of 10mg/kg/week by intraperitoneal injection, as previously described.[27] All experiments were conducted under IACUC approved protocols as we have previously described.[28] Mice were anesthetized with a mixture of ketamine 60mg/kg and xylazine 4mg/kg injected I.P., and fitted with a custom built external fixation device described previously. [24] Briefly, mice were implanted with two .028” diameter titanium pins implanted transcutaneously in the center of the 7^{th} and 10^{th} caudal vertebrae, and chronic compression of the flanked vertebrae was accomplished via four calibrated compression springs. This device was used to apply a compressive load equal to bodyweight (1X BW) or 6 times bodyweight (6X BW). The device was monitored to ensure maintained loading throughout the trial minimizing the effect stress relaxation due to soft tissue deformation or osteolysis. As controls, mice tails were instrumented with the device but without applying compressive load (0X BW). In the recovery and 1X BW experiments the chronic compressive load was applied for 8weeks. At 8 weeks the instrumentation was removed from the tails, mice were then either followed through recovery or sacrificed for tissue harvest. In the drug intervention experiments mice were continually loaded through 14 weeks, with treatments starting at the 8 week time point. The recovery and drug intervention groups were monitored through 14 weeks and then sacrificed.

Magnetic Resonance Imaging

Due to unacceptable metal artifacts, the custom external fixator was completely removed from the mice prior to, and replaced after, each MRI scan. MRI was performed on anesthetized mice using custom surface coils that were integrated into a clinical 3 Tesla Siemens Trio MRI (Siemens Medical Solutions, Erlangen, Germany) as previously described.[24] Briefly, the Pre-contrast MRI, and CE-MRI following retro-orbital injection of Gd-DTPA contrast agent (Omniscan, Amersham Health, Oslo, Norway) were performed using the pulse sequences and Osirix DICOM viewer analysis methods described previously.[28] The normalized marrow contrast enhancement (NMCE) was calculated by subtracting the signal intensity of the pre-contrast region of interest (ROI) circle (.65mm^2) from the same ROI in the post-contrast image, and then normalized for Gd-DTPA dosage variations by dividing this value by the contrast enhancement of a large section of muscle (>3mm^3) as previously described.[24;28]

Histology

The 6th through 11th caudal vertebrae were harvested at either 8 or 14 weeks and directly placed into 10% neutral buffered formalin for 36 to 48 hours for fixation. Specimens were then placed in 70% ETOH until micro-CT imaging 3–5 days later. The specimens were decalcified in 14% EDTA at room temperature (pH adjusted to 7.2) for 28 days. Specimens were then embedded in paraffin and 3μm sections were stained with alcian blue/Orange G (AB/OG). Histomorphometry to quantify the vascular sinus tissue area of the bone marrow (% sinus) and the cellularity of the bone marrow (mononuclear cells/mm^2) was then performed.

Statistical Analysis

A general linear repeated measures analysis of variance (ANOVA) model (Treatment, Duration, Treatment *Duration) was performed on resulting NMCE values for both vertebrae of each mouse included in each study. A Dunnett's post hoc analysis was used to determine significant differences between NMCE value means at each duration of compression and the baseline NMCE value mean. Pair-wise comparisons between groups at each time point were done with pooled t-tests and using the Bonferroni correction for multiple comparisons. A linear regression model using a least squares fit was used to correlate histomorphometry and NMCE values. All statistical tests were performed using SPSS Statistical Software (SPSS v17.0 Chicago, IL), all underlying assumptions of parametric methods were checked and no serious violations were detected. P-values less than 0.05 were considered significant.

RESULTS

Recovery from severe chronic compression

The tails of WT and TNF-Tg mice were instrumented to apply a 6X bodyweight for 8-weeks before removing the load. Consistent with previous observations,[24] the affected WT caudal vertebrae showed a significant increase in the NMCE values with as little as 2-weeks of loading, while no significant change was found in the TNF-Tg mice until week 8 (Figure 1A–C). Relieving this chronic compression resulted in a dramatic decrease in NMCE values in the WT mice, reducing them to near baseline levels 2 weeks later. Although the decrease in NMCE in TNF-Tg mice following release of the load was not as dramatic as WT, this bone marrow signal was significantly reduced to baseline levels within 6-weeks (Figure 1C). To better understand the nature of the NMCE changes following release of the load, we evaluated histology of the tails from these mice. The results suggested a return of fatty marrow in both strains, although the marrow of TNF mice was clearly more cellular than

WT (Figure 1D–G). Also apparent upon histological inspection is the soft tissue damage from chronic compression. The intervertebral discs of both the WT and TNF-Tg mice displayed compressed nucleus pulposus, the annulus appears disorganized, compressed, and asymmetric, and the distinction between the two regions along the lateral periphery was also poorly defined. Thus, these soft tissue changes are consistent with other models of DDD (Figure 1D–G).

Adaptive responses to a reduced compressive load

While our 6X BW model is designed to apply a significant chronic compression that induces permanent marrow changes, it is likely that the functional vertebral unit can adapt to less severe forces that result in acute changes. To test this, we applied a compressive load of 1X or 6X BW for 8 weeks to WT mice (Figure 2). As predicted, the 1X BW compression induced a transient increase in NMCE, which was significantly greater than baseline at 2, 4, and 6-weeks (Figure 2C). However, the signal intensity at 8 weeks was not significantly different from baseline NMCE values, or the average NMCE value of 0X BW WT tail vertebrae (0.31 ± 0.14) (mean± standard error), suggesting that this transient response is likely due to the adaptation of the tissue to the modest increase in load. In contrast, no adaptive response was observed in the WT vertebrae exposed to a chronic load of 6X BW, which induced a significant increase in NMCE that persisted throughout the study. Consistent with these MRI findings, histology of the tail vertebrae from these animals demonstrated the predicted increase in vascularity and cellularity in the 6X BW vs. 1X BW at 8-weeks (Figure 2D–G). Histology revealed a similar profile of the intervertebral disc in the 6X BW vs. 1X BW at 8-weeks, with disruption of the outer annulus, compression of the nucleus pulposus, and asymmetrical arrangement of the entire disc (Figure 2D–G).

TNF receptor signaling is required for the induction of compression-induced BME

We applied 6X BW to TNFR1&2−/− mice and compared it to 0X BW WT controls (Figure 3). Remarkably, both treatments failed to demonstrate any significant changes in NMCE at any time point, as the values remained below the 0.6 threshold level of BME throughout the study (Figure 3C). Consistently, histology of the bone marrow from these mice demonstrated similar vascularity and cellularity at 8-weeks (Figure 3D–G). Histology of the discs however show distinct differences between the unloaded and loaded discs. The unloaded intervertebral discs had fully expanded and seemingly well hydrated nucleus pulposus tissue. The annulus organization was well separated with distinct layers, and the separation between the two tissues was well defined with high proteoglycan content (Figure 3D). In contrast, the loaded discs showed tissue disruption and folding of the outer annulus, compression of the nucleus, decreased proteoglycan content, and an asymmetrical appearance (Figure 3F). Taken together, these data demonstrate that TNFR1&2−/− mice are completely resistant to compression-induced NMCE and bone marrow changes, suggesting that TNF signaling is required for this process to occur.

The effects of Anti-TNF therapy on chronic load-induced BME

We treated WT mice that had compression induced BME from 8-weeks of 6X BW with antibodies against TNF or an irrelevant IgG control (placebo) for an additional 6-weeks of continuous compression. Figure 4 demonstrates the results of this experiment in which no significant differences in NMCE values were observed between the anti-TNF and placebo groups. Interestingly, histology of the bone marrow from these animals displayed great variability in both the amount of sinus space present and its cellularity (data not shown), which we have not previously observed in mice studied for only 8-weeks. Although this observation confounds our ability to interpret the results of this 14-week study, the fact that anti-TNF therapy, at a dose known to ameliorate TNF-induced BME,[28] has no significant

effects on chronic compression-induced NMCE demonstrates that the presence of this inflammatory cytokine is not required to sustain this MRI signal or red marrow change.

NMCE correlates with marrow vascularity and cellularity

We performed regression analyses of the CE-MRI and histology data on marrow vascularity and cellularity. Figure 5 illustrates the significant correlations between these three outcome measures. Moreover, a multivariate regression analysis that combined marrow vascularity and cellularity demonstrated that these components account for 76% of the variability of NMCE.

DISCUSSION

Little is known about the origins of BME arising from non-traumatic incidence. The MRI appearance of increased intensity has been implicated in many varied instances including chronic inflammation associated with ASp[13], RA[29;30], osteoarthritis[31–33], and mechanical overload[34]. The ubiquity and ill-defined histopathology of these similar, but not necessarily biologically equal, findings complicate the interpretation of the MRI biomarker. Several questions arise regarding the similarities between such incidences of BME. Where does the cascade of events begin, the intervertebral disc, the endplate, the subchondral bone, the marrow compartment? Is the progression of degeneration and pain related to the incidence of BME? If BME can be halted or even reversed are the clinical symptoms in turn ameliorated? In order to begin answering such questions we have chosen to explore the inflammatory response elicited by overloading, and focus on the marrow compartment of the vertebrae. Several theories have been proposed as to the mechanism by which BME is produced; as a response to joint synovitis,[35] an increase in angiogenesis,[15] and/or a subclinical fracture prior to discernable fracture lines, also categorized as a stress fracture.[36] Previous models of DDD suggest that fractures at the endplate of the vertebrae can lead to DDD [37;38], which is likely to be secondary to osteoarthritic changes.[39] Microfractures that expose nuclear materials to the blood stream in the endplates of these vertebrae could be the inciting event that leads to BME formation. Exposure of tissue to cellular components of the nucleus pulposus have previously been shown to create a TNF-mediated inflammatory response that results in the recruitment of monocyte/macrophages.[40]

In the spine, the intervertebral disc likely performs its role as a shock absorber admirably even in the case of chronic overload, but the endplate and subchondral bone may well break down under this constant increased load, overtime leading to microfractures, resulting in the formation of BME. Previous experiments carried out in our lab have shown bone remodeling of the vertebrae in response to overloading, as evidenced by increased osteoclastic remodeling, and thickness changes in both trabecular and cortical bone.[24] While these experiments did not attempt to quantify the presence of microfractures the amount of remodeling indicates a profound effect on bony organization in response to the increased load. In experiments conducted on the human foot a wedged insert was placed into the shoe, BME formation was noted on MRI in as little as 2 weeks, at which point the wedge was removed and the BME resolved or greatly diminished by the 2 week follow up MRI.[34] Here we also find that BME induced by chronic vertebral overload is reversible upon removal of the overload. Further investigation of this response may shed light on the mechanism by which inflammatory mediators act in response to applied loads.

One of the most interesting phenomena of Modic changes is that they are not constant, and that as degeneration progresses, MT1 findings progress to MT2 and then ultimately to MT3 findings (in most observed cases).[7;9;41;42] The prevailing wisdom for the MT2 change is that the loading conditions on the bone have somehow changed alleviating the overload and leading to a fatty marrow conversion. This alleviation of load theoretically could arise from

internal compensation, such as changes in posture, architecture, or material properties of the supporting structures. The transient MRI findings of the vertebrae to a low level compression (1X BW), found in this study (Figure 3) are consistent with such a load compensation mechanism. This provides a great avenue for not only the initiation of the MT1 change, but also the investigation of the conversion to MT2 type changes.

Here we addressed the controversial role of TNF signaling in the development and maintenance of chronic compression-induced BME using genetic and pharmacological approaches in our model. The results clearly indicate a critical role for TNF signaling in the initiation of BME, as 6 X BW compression could not induce this MRI signal in genetically deficient mice that lack both TNFRI and TNFRII receptors. However, in contrast to our hypothesis that MT1 is maintained by the up-regulation and perpetual production of TNF, our failure to observe significant effects of anti-TNF therapy on NMCE and marrow vascular and cellular changes demonstrates that other factors must be present to mediate the persistence of BME. In an attempt to characterize TNF expression in compressed vertebrae, we performed real time RT-PCR on RNA isolated from the whole vertebrae of WT mice loaded through 8 weeks. The results of these experiments demonstrated that there is a significant decrease in the *tnf* mRNA levels, with respect to age matched controls (data not shown). This result is consistent with our other findings, and suggests that TNF is induced early following the traumatic insult of a significant compressive load. This TNF and resulting inflammatory cascade leads to the induction of BME. However, our findings that TNF is not continually expressed and that anti-TNF therapy does not affect chronic BME signals warrants future investigation to identify other factors. The tie between NMCE values and the marrow histomorphometry would appear to point to increased sinus space and increase vascular permeability. Previous work done in degenerative disc disease has shown an increase in angiogenic factors.[43;44] Candidates such as TGF-β and VEGF should be investigated to examine the role that vascularity and vascular permeability play in the MRI manifestation of BME.

The role of angiogenesis is a theoretical consideration in the manifestation of BME. An increase in the vascular supply as well as an increasingly “leaky” system in the marrow space is likely to manifest in the build up of fluid. Although the mechanism by which angiogenesis is stimulated by an increase in load is unknown, this increased vascularization is most likely due to down stream effects of the initial inflammatory response, which includes TNF. The critical role of vascularization in the radiological evidence of BME is apparent, as shown in the post-load histology found in the present study. Recovery from compression-induced edema formation is rapid and seems to be related to the decrease in sinus space rather than cellular infiltrate. An increased cellular state of the marrow is retained after the radiological evidence of BME is ameliorated, which is consistent with MT1 to MT2 changes. In the absence of another insult, the mononuclear cells cannot persist and the marrow would be expected to convert to MT3. Thus, we find that this animal model recapitulates many of the salient radiological and histological features of DDD, and could be useful to identify novel etiological factors responsible for spondyloarthropathy and evaluate potential interventions.

Acknowledgments

The authors would like to thank Ryan Tierney and Michael Thullen for technical assistance with the histology and micro-CT analyses respectively. This work was supported by Centocor Inc. and was supported by research grants from the National Institutes of Health PHS awards AR54041, AR48697, AI78907, AR56702 and ES01247.

Reference List

1. Deyo RA, Phillips WR. Low back pain. A primary care challenge. Spine (Phila Pa 1976). 1996; 21:2826–32. [PubMed: 9112706]
2. Carey TS, Garrett JM, Jackman AM. Beyond the good prognosis. Examination of an inception cohort of patients with chronic low back pain. Spine. 2000; 25:115–20. [PubMed: 10647169]
3. Deyo RA, Mirza SK, Turner JA, Martin BI. Overtreating chronic back pain: time to back off? J Am Board Fam Med. 2009; 22:62–8. [PubMed: 19124635]
4. Starr AM, Wessely MA, Albastaki U, Pierre-Jerome C, Kettner NW. Bone marrow edema: pathophysiology, differential diagnosis, and imaging. Acta Radiol. 2008; 49:771–86. [PubMed: 18608031]
5. Modic MT, Steinberg PM, Ross JS, Masaryk TJ, Carter JR. Degenerative disk disease: assessment of changes in vertebral body marrow with MR imaging. Radiology. 1988; 166:193–9. [PubMed: 3336678]
6. Modic MT, Masaryk TJ, Ross JS, Carter JR. Imaging of degenerative disk disease. Radiology. 1988; 168:177–86. [PubMed: 3289089]
7. Modic MT. Modic type 1 and type 2 changes. J Neurosurg Spine. 2007; 6:150–1. [PubMed: 17330582]
8. Braithwaite I, White J, Saifuddin A, Renton P, Taylor BA. Vertebral end-plate (Modic) changes on lumbar spine MRI: correlation with pain reproduction at lumbar discography. Eur Spine J. 1998; 7:363–8. [PubMed: 9840468]
9. Marshman LA, Trewhella M, Friesem T, Bhatia CK, Krishna M. Reverse transformation of Modic type 2 changes to Modic type 1 changes during sustained chronic low-back pain severity. Report of two cases and review of the literature. J Neurosurg Spine. 2007; 6:152–5. [PubMed: 17330583]
10. Khan MA. Update on spondyloarthropathies. Ann Intern Med. 2002; 136:896–907. [PubMed: 12069564]
11. Zhang X, Aubin JE, Inman RD. Molecular and cellular biology of new bone formation: insights into the ankylosis of ankylosing spondylitis. Curr Opin Rheumatol. 2003; 15:387–93. [PubMed: 12819465]
12. Manadan AM, James N, Block JA. New therapeutic approaches for spondyloarthritis. Curr Opin Rheumatol. 2007; 19:259–64. [PubMed: 17414952]
13. Braun J, Landewe R, Hermann KG, et al. Major reduction in spinal inflammation in patients with ankylosing spondylitis after treatment with infliximab: results of a multicenter, randomized, double-blind, placebo-controlled magnetic resonance imaging study. Arthritis Rheum. 2006; 54:1646–52. [PubMed: 16646033]
14. van der HD, Han C, DeVlam K, et al. Infliximab improves productivity and reduces workday loss in patients with ankylosing spondylitis: results from a randomized, placebo-controlled trial. Arthritis Rheum. 2006; 55:569–74. [PubMed: 16874778]
15. Appel H, Loddenkemper C, Grozdanovic Z, et al. Correlation of histopathological findings and magnetic resonance imaging in the spine of patients with ankylosing spondylitis. Arthritis Res Ther. 2006; 8:R143. [PubMed: 16925803]
16. Cohen SP, Bogduk N, Dragovich A, et al. Randomized, double-blind, placebo-controlled, dose-response, and preclinical safety study of transforaminal epidural etanercept for the treatment of sciatica. Anesthesiology. 2009; 110:1116–26. [PubMed: 19387178]
17. Genevay S, Viatte S, Finck A, Zufferey P, Balague F, Gabay C. Adalimumab in severe and acute sciatica: A multicentre, randomised, double-blind, placebo-controlled trial. Arthritis Rheum. 2010
18. Cohen SP, Wenzell D, Hurley RW, et al. A double-blind, placebo-controlled, dose-response pilot study evaluating intradiscal etanercept in patients with chronic discogenic low back pain or lumbosacral radiculopathy. Anesthesiology. 2007; 107:99–105. [PubMed: 17585221]
19. Karppinen J, Korhonen T, Malmivaara A, et al. Tumor necrosis factor-alpha monoclonal antibody, infliximab, used to manage severe sciatica. Spine. 2003; 28:750–3. [PubMed: 12698115]
20. Genevay S, Stingelin S, Gabay C. Efficacy of etanercept in the treatment of acute, severe sciatica: a pilot study. Ann Rheum Dis. 2004; 63:1120–3. [PubMed: 15115710]

21. Shin K, Lee S, Moon S, Min H, Park Y, Cho J, An H. A prospective, controlled trial of TNF alpha inhibitor for symtomatic patients with cervical disc herniation. Spine Jornal. 2005; 5(4):S45, 9–29. Ref Type: Abstract.
22. Tobinick E. Perispinal etanercept for neuroinflammatory disorders. Drug Discov Today. 2009; 14:168–77. [PubMed: 19027875]
23. LINDBLOM K. Intervertebral-disc degeneration considered as a pressure atrophy. J Bone Joint Surg Am. 1957; 39-A:933–45. [PubMed: 13438950]
24. Papuga MO, Proulx ST, Kwok E, et al. Chronic axial compression of the mouse tail segment induces MRI bone marrow edema changes that correlate with increased marrow vasculature and cellularity. J Orthop Res. 2010
25. Keffer J, Probert L, Cazlaris H, et al. Transgenic mice expressing human tumour necrosis factor: a predictive genetic model of arthritis. EMBO J. 1991; 10:4025–31. [PubMed: 1721867]
26. Pryhuber GS, Huyck HL, Bhagwat S, et al. Parenchymal cell TNF receptors contribute to inflammatory cell recruitment and respiratory failure in Pneumocystis carinii-induced pneumonia. J Immunol. 2008; 181:1409–19. [PubMed: 18606695]
27. Shealy DJ, Wooley PH, Emmell E, et al. Anti-TNF-alpha antibody allows healing of joint damage in polyarthritic transgenic mice. Arthritis Res. 2002; 4:R7. [PubMed: 12223110]
28. Proulx ST, Kwok E, You Z, et al. Elucidating bone marrow edema and myelopoiesis in murine arthritis using contrast-enhanced magnetic resonance imaging. Arthritis Rheum. 2008; 58:2019–29. [PubMed: 18576355]
29. Haavardsholm EA, Ostergaard M, Ejbjerg BJ, et al. Reliability and sensitivity to change of the OMERACT rheumatoid arthritis magnetic resonance imaging score in a multireader, longitudinal setting. Arthritis Rheum. 2005; 52:3860–7. [PubMed: 16320333]
30. Appel H, Loddenkemper C, Miossec P. Rheumatoid arthritis and ankylosing spondylitis -pathology of acute inflammation. Clin Exp Rheumatol. 2009; 27:S15–S19. [PubMed: 19822040]
31. Zanetti M, Bruder E, Romero J, Hodler J. Bone marrow edema pattern in osteoarthritic knees: correlation between MR imaging and histologic findings. Radiology. 2000; 215:835–40. [PubMed: 10831707]
32. Zhao J, Li X, Bolbos RI, Link TM, Majumdar S. Longitudinal assessment of bone marrow edema-like lesions and cartilage degeneration in osteoarthritis using 3 T MR T1rho quantification. Skeletal Radiol. 2010; 39:523–31. [PubMed: 20195865]
33. Kornaat PR, Bloem JL, Ceulemans RY, et al. Osteoarthritis of the knee: association between clinical features and MR imaging findings. Radiology. 2006; 239:811–7. [PubMed: 16714463]
34. Schweitzer ME, White LM. Does altered biomechanics cause marrow edema? Radiology. 1996; 198:851–3. [PubMed: 8628882]
35. Jimenez-Boj E, Redlich K, Turk B, et al. Interaction between synovial inflammatory tissue and bone marrow in rheumatoid arthritis. J Immunol. 2005; 175:2579–88. [PubMed: 16081832]
36. Woods M, Kijowski R, Sanford M, Choi J, De Smet A. Magnetic resonance imaging findings in patients with fibular stress injuries. Skeletal Radiol. 2008; 37:835–41. [PubMed: 18551292]
37. Adams MA, Freeman BJ, Morrison HP, Nelson IW, Dolan P. Mechanical initiation of intervertebral disc degeneration. Spine. 2000; 25:1625–36. [PubMed: 10870137]
38. Chow DH, Luk KD, Evans JH, Leong JC. Effects of short anterior lumbar interbody fusion on biomechanics of neighboring unfused segments. Spine. 1996; 21:549–55. [PubMed: 8852308]
39. Borenstein D. Does osteoarthritis of the lumbar spine cause chronic low back pain? Curr. Pain Headache Rep. 2004; 8:512–7.
40. Rand NS, Dawson JM, Juliao SF, Spengler DM, Floman Y. In vivo macrophage recruitment by murine intervertebral disc cells. J Spinal Disord. 2001; 14:339–42. [PubMed: 11481557]
41. Kjaer P, Korsholm L, Bendix T, Sorensen JS, Leboeuf-Yde C. Modic changes and their associations with clinical findings. Eur Spine J. 2006; 15:1312–9. [PubMed: 16896838]
42. Marshman LA, Metcalfe AV, Krishna M, Friesem T. Are high-intensity zones and Modic changes mutually exclusive in symptomatic lumbar degenerative discs? J Neurosurg Spine. 2010; 12:351–6. [PubMed: 20367371]

43. Kato T, Haro H, Komori H, Shinomiya K. Sequential dynamics of inflammatory cytokine, angiogenesis inducing factor and matrix degrading enzymes during spontaneous resorption of the herniated disc. J Orthop Res. 2004; 22:895–900. [PubMed: 15183452]

44. Tolonen J, Gronblad M, Virri J, Seitsalo S, Rytomaa T, Karaharju E. Transforming growth factor beta receptor induction in herniated intervertebral disc tissue: an immunohistochemical study. Eur Spine J. 2001; 10:172–6. [PubMed: 11345640]

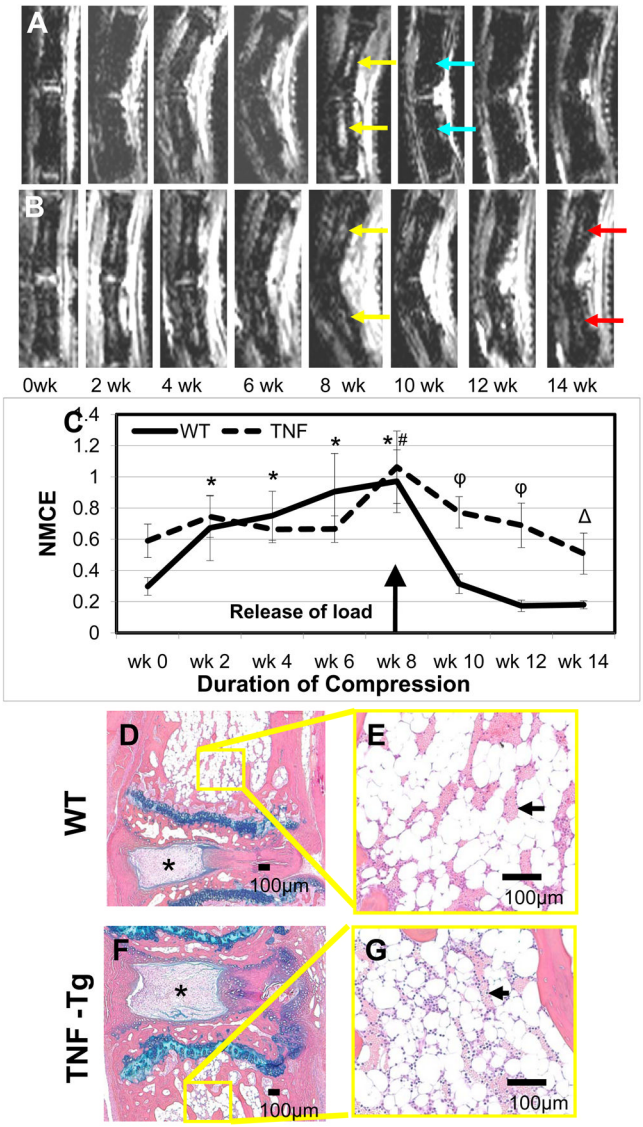

Figure 1. Recovery from compression induced BME after release is rapid in WT but not TNF-Tg mice

Representative longitudinal series of caudal vertebrae post-contrast CE-MRI in 6X BW WT (A) and 6X BW TNF-Tg (B) mice showing increase in signal intensity after 8 weeks of compression (yellow arrows). Note that 2 weeks after release of the load the BME of WT was back to baseline (blue arrows), however the BME in TNF-Tg mice was retained through14 (red arrows). Quantification of normalized contrast enhanced intensity (NMCE) values (C) illustrates the intensity changes associated with compression, means and standard errors (SE) are shown (n=4 tails; 8 vertebrae for each group). (**p<.05 WT vs. TNF-Tg at baseline; * p<0.05 WT at each time point vs. WT at wk 0; # p<0.05 TNF-Tg at each time point vs. TNF-Tg wk 0; ϕ p<0.05 WT vs. TNF-Tg at each time point). Representative AB/OG stained sections of the experimental caudal vertebrae and herniated disk (*) at 14 weeks shown at 5X magnification (D,F), and 20X magnification (E,G). Note the similarity in vascular sinus area (arrows: WT 21.7 ± 12.3% vs. TNF-Tg 27.2 ± 5.1%, p=0.22), while the TNF-Tg marrow is more cellular vs. WT (WT 2972 ± 741 cell/mm^2 vs. TNF-Tg 3673 ± 1476 cell/mm^2, p< 0.05).

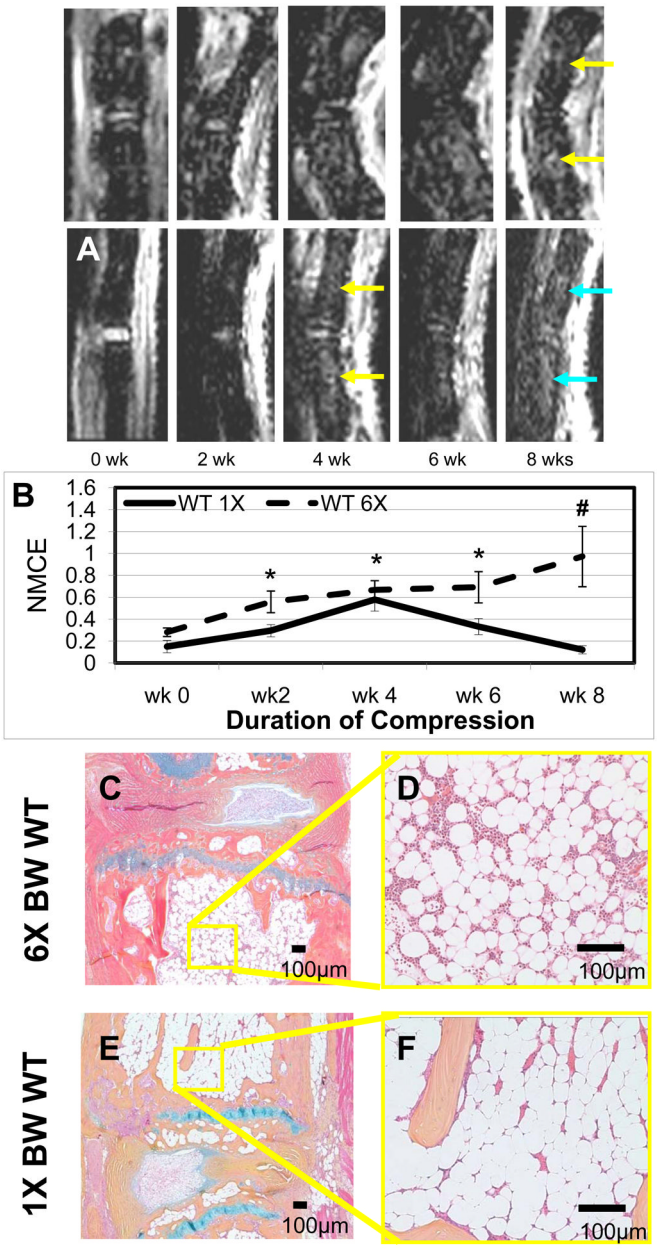

Figure 2. Chronic compression at 1X BW induces transient marrow changes that resolve within 8 weeks

Representative longitudinal series of caudal vertebrae post-contrast CE-MRI in a 6X BW WT (A) and 1X BW WT (B) mice. Note that the BME in the 6X from 4 through 8 weeks (yellow arrows), while the BME in the 1X at 4 weeks (yellow arrow) resolved on its own at 6 and 8 weeks (blue arrow). Quantification of NMCE (C) illustrates the intensity changes associated with compression over time, means and standard errors (SE) are shown (n=5 tails; 10 vertebrae for each group) (*$p<0.05$ vs. wk 0; #$p<0.05$ vs. 1X at wk8). Representative AB/OG stained sections of 6X BW WT(D,E) and 1X BW WT (F,G) mice at 8 weeks taken at 5X magnification (D,F) and 20X magnification (E,G). Note the significant differences in both vascular sinus area (1X 13.4 ± 3.9% vs. 6X 35.0 ± 3.0%, $p<0.01$), and cellularity (1X 1886 ± 884 cell/mm^2 vs. 6X 3265 ± 235 cell/mm^2, $p<0.01$).

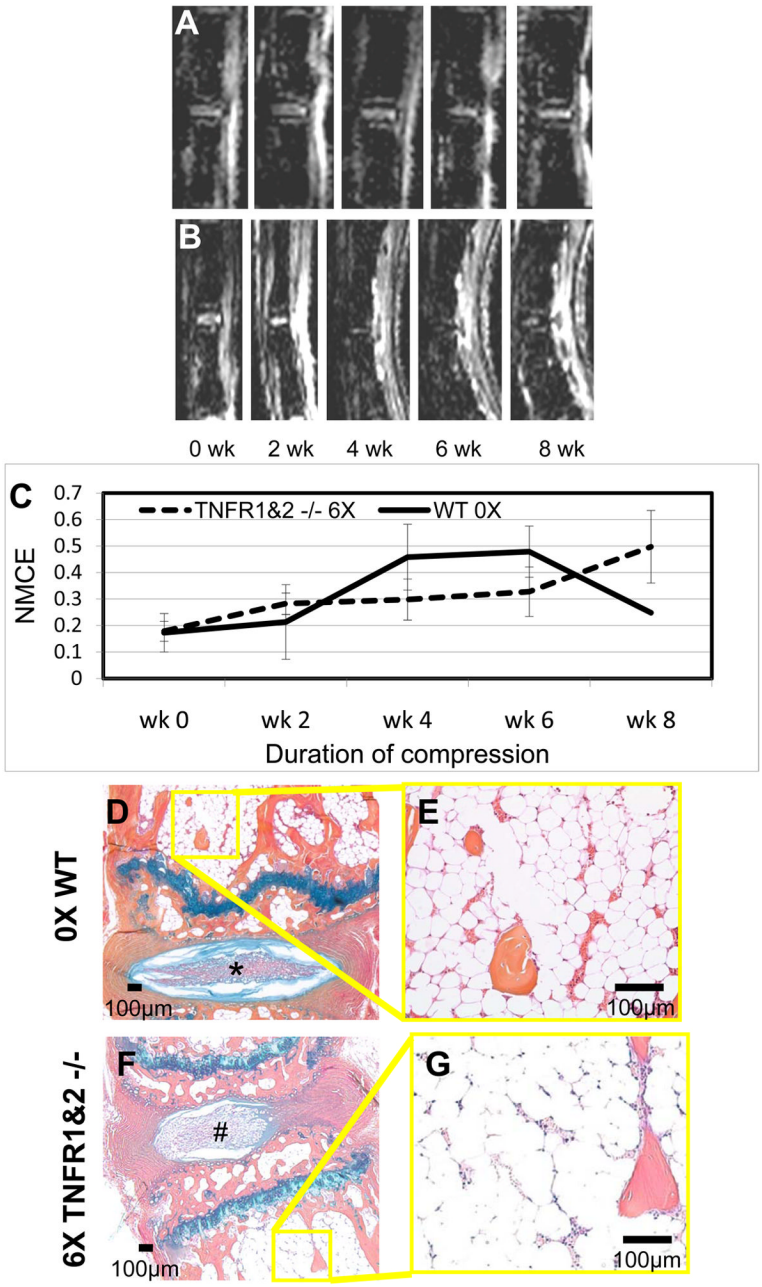

Figure 3. Chronic compression of TNF-receptor knockout at 6X BW fails to induce BME

Representative longitudinal series of caudal vertebrae post-contrast CE-MRI in 0X BW WT (A) and 6X BW TNFR1&2−/− (B) mice show no increase in signal intensity through 8 weeks of compression. Quantification of NMCE (C) illustrates the intensity changes associated with compression, mean and standard errors (SE) are shown (n=4 tails; 8 vertebrae for each group). Note that neither treatment achieved a NMCE signal at the 0.6 threshold for BME (dotted line) at any time point. Representative AB/OG stained sections of 0X BW WT (D,E) and 6X BW TNFR1&2−/− (F,G) mice at 14 weeks following release of load at 5X magnification (D,F), and 20X magnification (E,G). Note the normal disk in the 0X (*) vs. the herniated disk in the TNFR1&2−/− (#), and the similarities in both vascular

sinus area (0X 18.9 ± 3.8% vs. TNFR1&2−/− 14.7 ± 2.0%), and cellularity (0X 1597 ± 684 cell/mm^2 vs. TNFR1&2−/− 2490 ± 708 cell/mm^2).

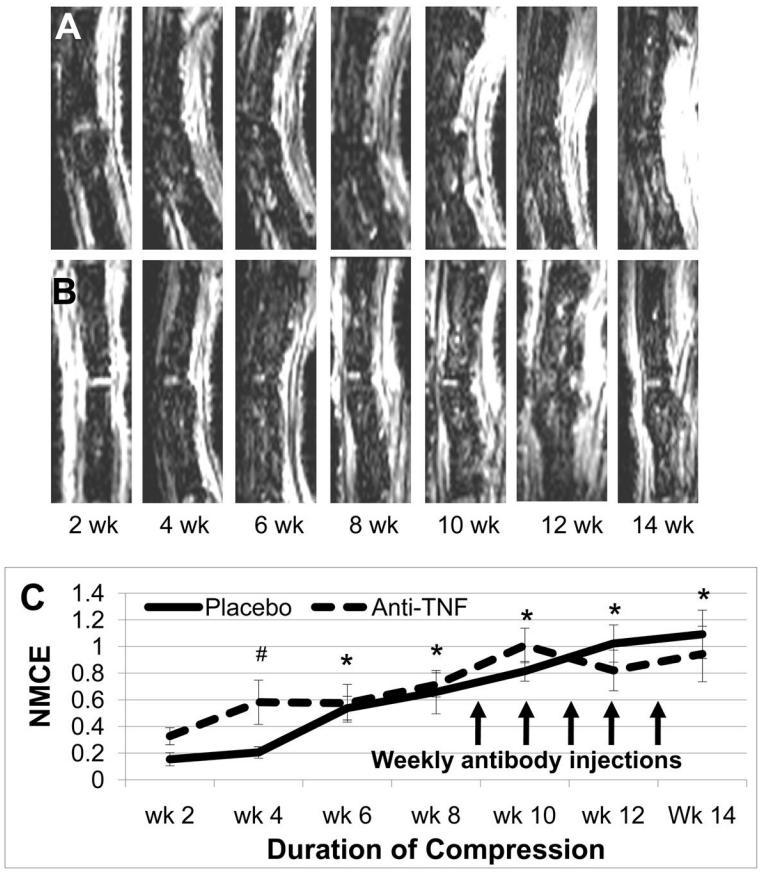

Figure 4. Anti-TNF therapy fails to relieve compression induced BME

Representative longitudinal series of caudal vertebrae post-contrast CE-MRI in placebo treated 6X BW WT (A) and anti-TNF treated 6X BW WT (B) mice showing increase in signal intensity through 14 weeks of compression. Quantification of NMCE (C) illustrates the intensity changes associated with compression, means and standard errors (SE) are shown (n=4 tails; 8 vertebrae for each group). Arrows indicate weekly injections of placebo or anti-TNF treatment (* $p<0.05$ vs. wk 0 for both groups; # $p<0.05$ vs. wk 0 for anti-TNF).

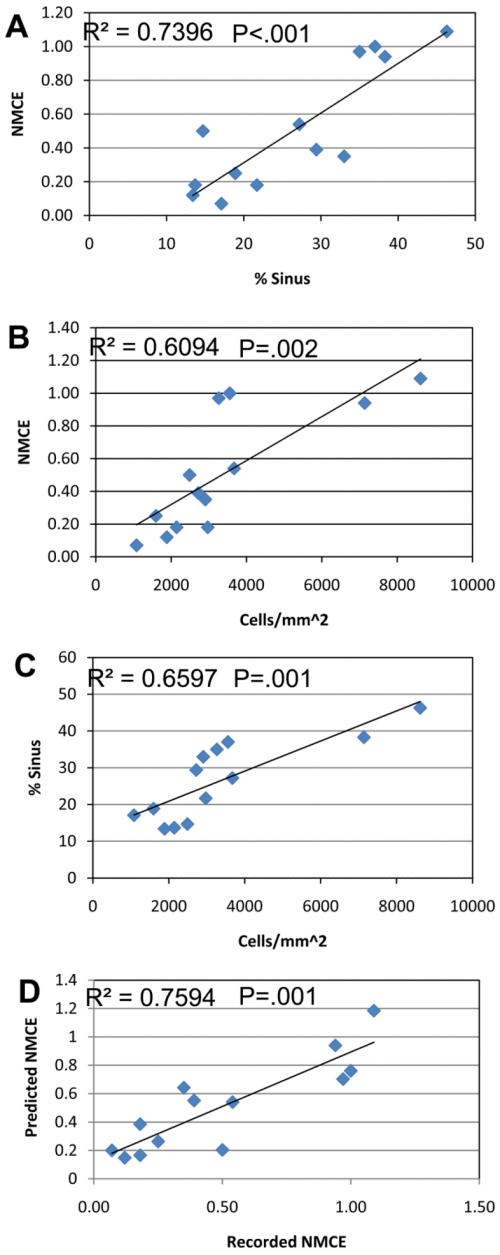

Figure 5. Correlation of marrow vascularity and cellularity with NMCE

The mean values of the 13 experimental groups in this study were used to estmate linear regression models for NMCE vs. vascularity (% vascular sinus tissue area) (A); NMCE vs. cellularity (B); vascularity vs. cellularity (C); and a multivariate regression model including both vascularity and cellularity as covariates (predicted NMCE) vs. NMCE (D). The significance of these correlations is indicated by their R^2 and P values.